Statistical Analysis of Historical SEL Test Data to Provide A Priori Risk Estimates for Use of Unhardened CMOS Parts

Ray Ladbury, *Member, IEEE*, Gregory R. Allen, *Member, IEEE,* Farokh Irom, *Member, IEEE*, Razvan Gaza, *Member, IEEE*, Sergeh Vartanian, *Member, IEEE*, Jonathan D. Barth, *Member, IEEE,* Robert F Hodson

***Abstract*— SEL is a serious obstacle to use of state-of-the-art microelectronics, and a priori prediction of SEL susceptibility has proven elusive. We develop SEL risk-assessment tools based on analysis of large archives of SEL test data for unhardened CMOS parts. Results include a flexible method for bounding SEL rates even with minimal test data.**

***Index Terms*— Single-event effects, single-event latchup reliability estimation, quality assurance; statistical techniques**

I. Introduction

Single-Event Latchup (SEL) remains a persistent and difficult obstacle to the confident use of state-of-the-art microelectronics in high-radiation environments. Even parts not fabricated mainly in Complementary Metal-Oxide-Semiconductor (CMOS) may be vulnerable due to CMOS control logic, Input-Output (IO), etc. Improving the odds by *a priori* prediction has proved difficult because there are no consistent trends with respect to vendor, process, function, etc. [1-7]. Screening with protons (useful for revealing common nondestructive Single-Event Effects (SEE) [8]) is often ineffective due to the short ranges of proton recoil ions and the deep sensitive volumes (SV) typical of SEL [9-12]. The difficulty of predicting SEL susceptibility is unfortunate, because SEL behavior is highly variable and can pose significant threats to part and system reliability. Roughly half of unhardened CMOS parts are SEL susceptible, and in 50% of these parts, SEL can be destructive [4]. SEL rates vary across more than 6 orders of magnitude, with a few percent of parts having rates exceeding one per month even in relatively benign radiation environments [5-7]. When SEL is not destructive, it can result in latent damage [13,14] that degrades subsequent reliability, and even if truly nondestructive, SEL requires disruptive intervention, such as cycling power to the device. Also, the most common circuit-level mitigation—a monitoring circuit to protect against overcurrent and cycle power to recover functionality—may be unwieldy or ineffective due to the variability of SEL response and the need to ensure that it protects against latent damage as well as catastrophic failure. The detection circuit can also produce spurious resets due to single-event transients in the detection circuitry [15-17].

An alternate approach to prediction via part similarity involves analyzing datasets with as broad a variety of SEL susceptible parts as possible. Such analyses can yield insights into the likelihood a generic unhardened CMOS part will exhibit SEL, whether SEL is likely to be nondestructive or destructive and whether these proportions differ for different part types, vendors, processes, etc. [4]. They can also be used to examine variability in SEL rates or in the fit parameters to SEL cross section (σ) vs. Linear Energy Transfer (LET) curves that determine rates [5,6]. Moreover, understanding part SEL response in historical tests can provide guidance for how to investigate gaps in our current understanding, such as dealing with the threat of latent damage for parts where SEL is not immediately destructive [13,14].

The types of analyses that can be carried out with a broad dataset of part SEL susceptibilities depend on the quality of the data. If a dataset contains a large proportion of go/no-go tests at only a few LET values, it will likely be impossible to accurately estimate SEL rates or fit parameters for the cross section vs. LET. On the other hand, if the database includes data only for parts that are SEL susceptible, it will not be possible to estimate *a priori* how likely an average unhardened CMOS part is to be SEL susceptible or how likely an SEL is to be destructive. However, when different databases are analyzed together, the results can often be used to quantify and compensate for shortcomings and biases in each dataset, presenting a fuller picture of the risks posed by a potentially susceptible device in a hardware design.

Here, we perform statistical and trend analyses on large datasets of SEL susceptible parts to develop methods for bounding SEL rates in such parts and to map out strategies to fill gaps in current knowledge. One of the datasets used for this analysis was compiled by researchers at CERN and published

Manuscript received July 15, 2024. The authors thank the Human Landing Systems program and the NASA Engineering and Safety Center for supporting this research.

R. Ladbury is with NASA Goddard Space Flight Center, Greenbelt, MD 20771, USA (phone: 301-286-1030, e-mail: raymond.l.ladbury@nasa.gov.

Greg R. Allen is with the Jet Propulsion Laboratory, California Institute of Technology Pasadena, CA 91109 (USA), phone: 818-393-7558, e-mail: grallen@jpl.nasa.gov

Farokh Irom is with the Jet Propulsion Laboratory, California Institute of Technology Pasadena, CA 91109 (USA), phone: 818-354-7463, e-mail: farokh.irom@jpl.nasa.gov.

Razvan Gaza is with Johnson Space Center, Houston, TX 77056 (USA), phone: 281-244-2412, e-mail: razvan.gaza@nasa.gov

Sergeh Vartanian is with the Jet Propulsion Laboratory, California Institute of Technology Pasadena, CA 91109 (USA), phone: 818-354-0311, e-mail: sergeh.vartanian@nasa.gov

Jonathan D. Barth is with NASA Goddard Space Flight Center, Greenbelt, MD 20771 (USA), phone: 301-286-5966, e-mail: jonathan.d.barth@nasa.gov.

Robert F. Hodson is with NASA Langley Research Center, Hampton, VA 23666 (USA), phone: 757-864-2326, email: robert.f.hodson@nasa.gov

by permission of the compilers (Ruben Garcia-Alia and Andrea Coronetti) in [7], where it was used to develop prior probability distributions for SEL rates. We also use the database of SEL tests performed by the Jet Propulsion Laboratory (JPL), augmenting previous results [4]. We begin by discussing the datasets and analysis methods. We then report results for analysis of both the CERN and JPL databases, extracting trends and providing guidance for use of the dataset to assess SEL risk. We then show that complementary aspects of these databases can strengthen the conclusions arising from each.

II. SEL DATASETS AND METHODOLOGY

The two datasets used in this analysis include several different types of data in varying amounts. The CERN dataset includes data drawn from several sources for over 80 different part types. The full dataset was published [7] (to which, for brevity's sake, we refer the reader for details) in 2023, along with the original references of the data. Although some of the entries in this database are go/no-go SEL tests at a single qualifying LET level, over 50 of the entries have sufficient data for determining the onset LET (LET_0) and limiting cross section (σ_s), and over 30 of the part types include sufficient data to determine a full Weibull fit to σ vs. LET. This allows correlation- and trend- analyses between Weibull fit parameters to be performed. Examples of how such trends can be applied are given in [7] and will be further developed below.

The other dataset consists of test reports on SEL susceptibility for hundreds of potentially susceptible parts, which were produced during part qualification for use in missions operated by JPL. Because many of the SEE tests were carried out solely to qualify parts for JPL missions, they have too few cross-section points for a Weibull fit, or, in some cases, even to determine σ_s and LET_0. The LET of the test ion used varied depending on the requirements for the mission. However, even such limited data can be useful—for example, in estimating the susceptibilities of CMOS devices typically used for JPL missions to destructive or nondestructive SEL [4]. We update these analyses using the more recent test results (2016-2023), increasing statistics for the analyses and allowing invetigation of any trends in susceptibility over time.

The analyses are exploratory—looking for trends in the data that may be useful for a priori estimation of risks arising from SEL susceptibility in unhardend CMOS parts. However, the datasets are complementary, with the CERN data often being sufficient to determine at least some Weibull fit parameters allowing correlation studies and model development. On the other hand, the shear numbers of parts and the variety of part types in the JPL dataset—along with the inclusion of both positive and negative tests for SEL susceptibility—facilitates assessments of potential risks for a "generic" unhardened CMOS part likely to be of interest for NASA missions.

III. RESULTS: CERN DATASET

Although the CERN dataset allows estimation of at least some Weibull fit parameters for σ vs. LET, some caveats are in order for dealing with such data generally. Many Weibull fits are bounding fits for hardness assurance purposes rather than best parametric estimates. Such a bounding fit tends to overestimate σ_s and underestimate LET_0 as well as the Weibull width w an shape s. Moreover, the extent of the conservatism varies from one radiation analyst to another and may be different for different parts even for the same analyst, depending on the criticality of the part application. While this can introduce systematic uncertainties into parametric estimates, we refit σ vs. LET when data were available. Also, even when only parametric estimates were given, fitting is at least guided by the data. As such, large errors are unlikely and any residual errors are unlikely to introduce spurious trends.

Fig. 1 shows histograms of the fit parameters (57 parts for LET_0 and σ_s and 31 for w and s). Because σ_s spans 6 orders of magnitude, we have histogrammed $\ln(\sigma_s)$. We have also calculated the 6 correlation coefficients for each pair of the 4 Weibull fit parameters (see Table I). Of these, only the correlation between LET_0 and σ_s (-0.23) and that between Weibull width and shape (-0.42) exceeded 0.2 in magnitude.

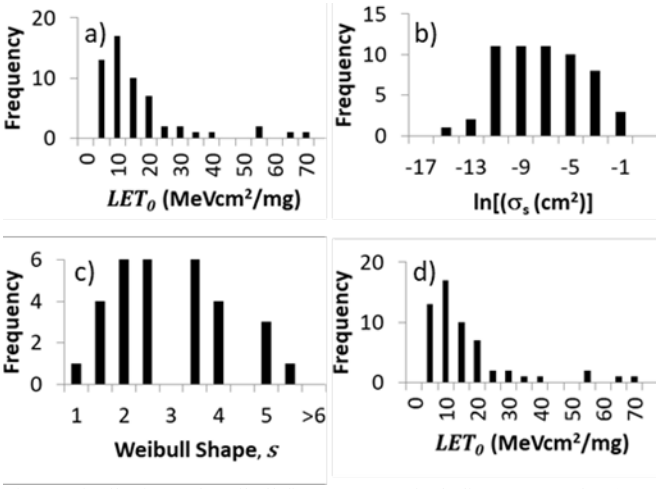

Fig. 1. Distributions of Weibull fit parameters, including 57 parts for a) onset (LET_0) and b) saturation ($\ln(\sigma_s)$); and 31 parts for (c) Weibull shape, s, and (d) Weibull width, w.

TABLE I: WEIBULL FIT PARAMETER CORRELATION MATRIX

	LET_0	σ_s	w	s
LET_0	—	—	—	—
σ_s	-0.23	—	—	—
w	-0.07	-0.16	—	—
s	0.11	-0.05	-0.42	—

Figs. 2 and 3 illustrate the LET_0-σ_s and w-s correlations, respectively. Fig. 2is best fit with a power law trend. This means that the trend for σ_s can be expressed in terms of LET_0:

$$\sigma_s \sim 0.012 * LET_0^{-1.82} = \exp\left(m_{ln}(LET_0)\right) \quad (1)$$

or that for LET_0 can be expressed in terms of σ_s:

$$LET_0 \sim 1.96\sigma_s^{-0.192} = \exp\left(m_{ln}(\sigma_s)\right) \quad (2)$$

Ref [7] found variation about the trend could be modeled with a lognormal (LN) model with constant LN standard deviation s_{ln} and the trend ((1) or (2)) as a median. Since the

lognormal mean is the logarithm of the median, the LN mean (m_{ln}) is just the log of (1) for the distribution of σ_s given LET_0:

$$P(\sigma_s \mid LET_0)=LN(m_{ln}(LET_0),s_{ln}) \quad (3)$$

where the best fit s_{ln}=2.545. Similarly, for the distriubution of LET_0 given σ_s, m_{ln} is the logarithm of (2) above:

$$P(LET_0 \mid \sigma_s)=LN(m_{ln}(\sigma_s),s_{ln}) \quad (4)$$

and s_{ln} for (4) is 0.82. Using (3) and (4), if we know either σ_s or LET_0, we can bound the other at a desired confidence (CL).

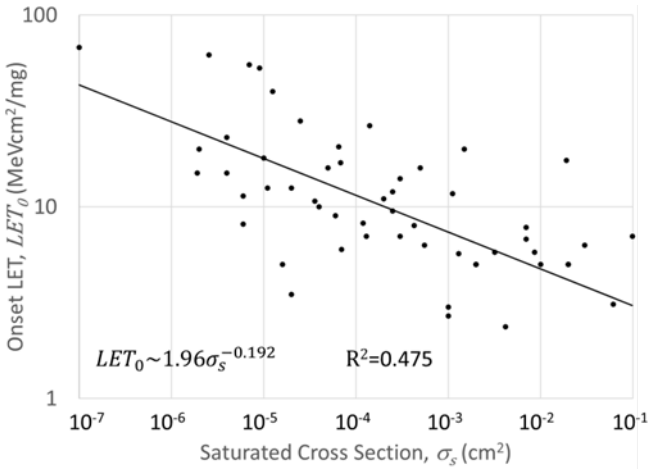

Fig. 2. The correlation between LET_0 and σ_s follows a power law, which persists over >100x in LET_0 and 6 orders of magnitude in σ_s.

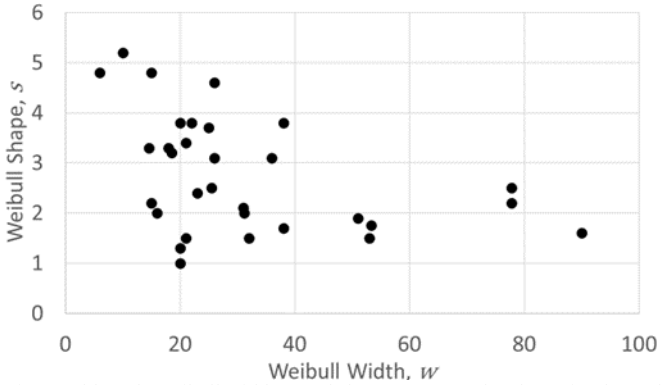

Fig. 3. Although Weibull width w and shape s are correlated, no simple model relates the two. The correlation means they cannot be treated as independent.

Because the trend does not constrain the increase of σ vs. LET, rate estimation is impossible. However, w=0 gives a worst-case σ vs. LET (step function at LET_0 from 0 to σ_s):

$$R_{FOM} = C_E \times {}^{\sigma_s}/_{(LET_0 + w(0.288)^{1/s})^2} < C_E \, {}^{\sigma_s}/_{LET_0^2} \quad (5)$$

where R_{FOM} is the figure of merit (FOM) rate estimate [18] and C_E is rate constant for the environment. The conservatism in this bounding rate, R_B, will be discussed below.

Although the trend between w and s in Fig. 3 is evident, it does not lend itself to a simple model. However, it means that w and s cannot be treatied independently. In [7], this was resolved by sampling w-s pairs from the 31 parts in the dataset.

It is useful to view these correlations in terms of the effect they have on the Weibull fit and the resulting rate. The negative correlation between LET_0 and σ_s means parts with low LET_0 will likely have high σ_s, and therefore very high rates, while high-LET_0 parts likely have very low rates. The effect of the inverse correlation between Weibull width w and shape s is more subtle. High values for both w and s lower rates by diminishing the cross section near onset where ion fluxes are highest. For this reason, and because w and s cannot be treated independently, in section VI, we examine the combined effect for w-s pairs in Fig. 3 on rate relative to the bound given in (5).

IV. Results: JPL Dataset

Because the JPL dataset includes test reports for hundreds of different part types and is increasing all time, analysis of this dataset is still ongoing. As noted above, much of the data were gathered in the course of parts radiation qualification for NASA missions, and so may only consist of a go/no-go test to a required LET (e.g. 37 MeVcm²/mg for risk-tolerant missions or >75 MeVcm²/mg for high-value missions). It is most useful to view such tests as a binomial trial with two possible outcomes "Susceptible" and "Not Susceptible," at the highest test LET. (We discuss the implications of the variable test LETs below.) The data are also broken up into tranches corresponding to various years—e.g. pre-2008, 2010-2015 and post 2015. This makes it possible to examine whether SEL susceptibilities exhibit trends over these time intervals. This is not necessarily the same as looking at trends in technology, as even the latest years likely include parts manufactured over a broad range of CMOS dimensions. Part functions are also included in the database, allowing comparison of the proportions of SEL susceptibility from one part function to another. In examining these trends, it is important that the samples not be divided too finely, because binomial statistics converge slowly with sample size. As such, we divide the parts into 4 time periods: pre-2012, 2012-2015, 2016-2019 and 2020-2023 (see fig. 4). The time-series from pre-2012 to 2023 shows no statistically significant variation in the proportion of parts that are SEL susceptible, remaining near 50% for all periods assessed.

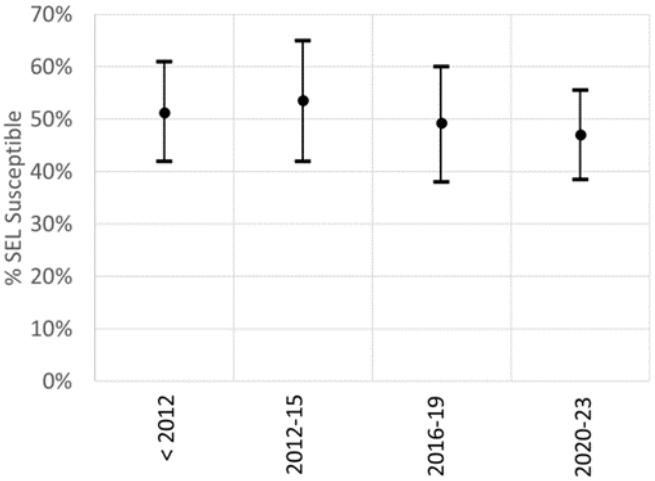

Fig. 4. The percentage of unhardened CMOS parts susceptible to SEL has shown no statistically significant change in over 20 years. Circles show best estimate and error bars 90% confidence interval.

We also divide the data into 7 different broad functional categories: Analog-to-Digital/Digital-to-Analog Converters (ADC/DAC), Field Programmable Gate Arrays (FPGA), Power Devices (Voltage/Power Regulators, Converters and Supervisors, etc.), Amplifiers (Operational, Instrumentation, etc.), Processors (microprocessors, digital signal processors, microcontrolers, etc.), High-Density Memory (mainly Dynamic Random Access and FLASH memories), and Miscellaneous (Drivers, Logic and other device types where statistics do not permit reliable estimation). Susceptibility by function (Fig. 5) is more interesting, showing ADC/DAC with significantly higher SEL susceptibility (>70% versus ~50% over all CMOS parts). Amplifiers and high-density memories show slightly lower susceptibilities. A similar analysis shows no significant variation in % susceptibility from one vender to another.

Qualitative Observations: Some test reports in the database note that the parts failed due to SEL despite current limiting and SEL detection circuitry, suggesting that mitigation of SEL threats via such methods may not be possible for all parts (which will not be known without heavy-ion test data). Ref. [4] found that roughly 50% of SEL susceptible parts latched up destructively. The high proportion of go/no-go tests in which destructive SEL susceptibility may not be investigated has prevented us from updating this result, although the consistency across time for overall SEL susceptibility suggests it will not have changed significantly. There is also evidence that latent damage remains an issue, as some parts continued working after several SELs but then abruptly failed—completely or partially.

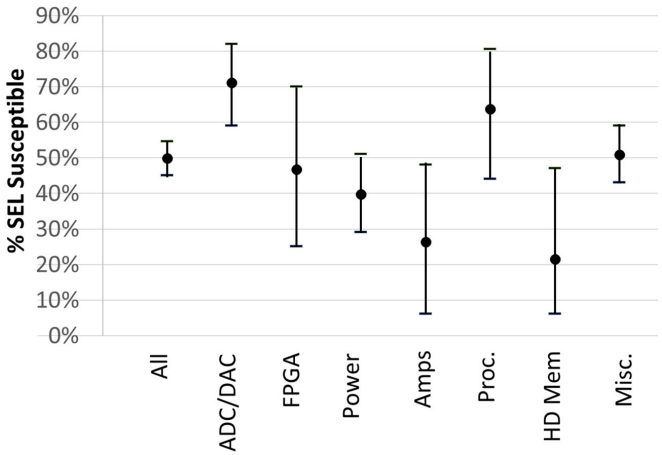

Fig. 5. Percent of SEL susceptible parts remains consistent across part functions at ~50%, with only ADC/DAC significantly higher and amplifiers and HD Memories perhaps somewhat lower.

V. Cross-Checking and Validating Datasets

Although the datasets examined here include different types of data, the use of them to predict risk due to SEL susceptible parts is predicated on them portraying a consistent picture of SEL across databases. Validation of this assumption is important, but it also provides an opportunity to correct for known biases in different datasets. One of the shortcomings of the JPL dataset is that many of the parts were tested only to moderately high LET (e.g. 42.6, 37 or even 26 MeVcm^2/mg), leaving open the question of how likely such a test is to miss a part that would have been SEL susceptible at higher LET—and thereby underestimating the proportion of SEL susceptible parts. However, the distributions from fig. 1 can correct for such biases if we consider the parts therein to be representative of SEL susceptible parts. Fig. 6 shows the data in Fig. 1a) as a quantile plot of the % of parts (Q) with LET_0 below the LET value on the abscissa. Multiplying the number of SEL-free parts tested only up to the abscissa value by the corresponding (1/Q-1), one can correct the proportions in figs. 4 and 5 for parts that would have latched up at higher LET values (e.g. for LET_T=26 MeVcm^2/mg, one multiplies by 1/0.86-1~0.16). Doing this for all parts tested to LET<60 MeVcm2/mg, the proportions change by <3.5%. Fig. 6 is also useful for test planning and risk assessment for potentially susceptible parts.

Similarly, although a large proportion of the entries in the JPL database are go/no-go qualification tests at one or a few LET values, a few have sufficient measurements of σ vs. LET to provide independent measurements of both σ_s and LET_0. These can be examined to determine whether they are consistent with the lognormal/power-law-trend model derived from the CERN dataset. Table 2 makes this comparison for the 11 parts from the JPL database for which this is possible by listing the best-fit LET_0 versus that predicted (median) by the model. As can be seen, the observed LET_0 for all but 1 of the 11 part types from the JPL database are bounded by the 90% confidence interval, and that one falls within the 92% interval. Six of the 11 parts fall quite close to the median/predicted value.

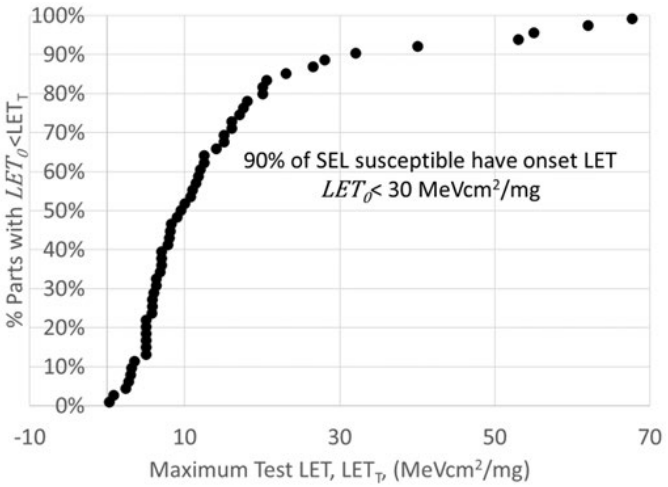

Fig. 6. Data in Fig. 1a presented as a percentile plot can be used both for test planning and for estimating the chances that a part would latchup at LETs greater than the highest test LET.

These independent data support the predictive power and utility of the model ((3) and (4), above) derived from the CERN data.

VI. Less Conservative Rate Estimates

As noted above, the SEL rate bound in (5) is likely to be very conservative because it assumes worst-case behavior for σ vs. LET constrained by the values of σ_s and LET_0. (step function). In [7] the conservatism was estimated for the system-level bounding method by assuming the 31 *w-s* pairs in Fig. 3 are representative of the sorts of behavior likely to occur for SEL. Here we examine whether a similar assumption can be used to bound SEL rates for a desired confidence rather than worst case.

Table II: Performance of Predicted vs. Observed LET_0

Part #	σ_{obs}	Mfg.	Func.	Obs. LET_0	Med. LET_0	90%WC LET0	P($LET_0 \leq$ Obs.)
AD9283	5.0E-07	ADI	ADC	>29.8	31.70	11.10	47%
Blackjack	1.0E-02	LSI	ASIC	>5	4.47	1.66	53%
NB3N2304NZ	2.5E-04	ON Semi	Buffer	8	15.10	5.20	22%
AD7760	5.0E-04	ADI	ADC	8	8.43	2.95	47%
LTC1864	8.0E-05	LTC	ADC	8.5	11.99	4.19	34%
LMG1210	5.0E-05	TI	Driver	12	13.12	4.59	45%
ADP195	8.0E-07	ADI	Switch	>20.3	29.03	10.15	>33%
CC1200	5.0E-04	TI	XCVR	2.7	8.43	2.95	8%
Snapdragon LPDDR5	1.0E-03	QCOM	Emb. DDR	<14.3	7.38	2.58	<79%
MAX2982	9.0E-03	Maxim	XCVR	5	4.84	1.69	49%
MAX2981	1.0E-05	Maxim	FE Line Drvr.	16	17.88	6.25	45%

ADI=Analog Devices, Inc., LSI=LSI Logic Corp., LTC=Linear Technology Corp. (Now ADI), Maxim=Maxim Integrated (Now ADI), ON Semi=ON Semiconductor Corp., QCOM=Qualcomm, Inc., TI=Texas Instruments

To ensure independence from the CERN dataset (the basis for the representative *w*-*s* dataset), we begin with the 11 parts from the JPL dataset listed in Table II. We estimate R_{FOM} for the measured σ_s and predicted LET_0 and each *w*-*s* pair in Fig.3, as well as the bounding rate given in (5). Dividing each R_{FOM} by R_B produces 31 rate ratios, $r = R_{FOM}/R_B$, between 0 and 1. Figs. 7a)-7c) give quantile plots (ordered smallest to largest with quantile assigned), along with best fits to a β distribution. The beta distribution is flexible for fitting data defined between 0 and 1, and gives a measure of how well behaved (e.g., unimodal, decreasing to 0 at 0 and 1, etc.) the distribution is:

$$\beta(r) = \left(\frac{\Gamma(\alpha)\Gamma(\beta)}{\Gamma(\alpha+\beta)}\right)^{-1} \times r^{\alpha}(1-r)^{\beta} \qquad (0 \leq r \leq 1) \qquad (6)$$

where α, β>0 and Γ(-) is the gamma function of the argument.

The β fits in Fig. 7 are very good (worst Kullback-Liebler divergence between data and fit <0.05 and the worst-case R^2>0.97), suggesting that the distributions are well behaved. The bounding rate in (5) is most conservative when LET_0 is small (>100x for large *w*), as expected given the dependence of R_{FOM} on *w*, LET_0 and *s*. With increasing LET_0 the distribution moves to the right and becomes broader, and the level of conservatism for the bounding rate may be less than ~2-3x. If one wishes to bound the SEL rate less conservatively than the bound in (5), one can do so nonparametrically by interpolating between the two FOM rates bounding the desired confidence below and above. However, given the good fits of the beta distributions, one could equally divide by *r* corresponding to the desired confidence for the appropriate beta distribution. Moreover, for $4 \leq LET_0 \leq 40$ MeVcm^2/mg, the fit parameters for the beta distribution follow power laws in LET_0 to an excellent approximation (see fig. 8). This procedure allows the *w*-*s* data from the CERN dataset to be used to provide more realistic bounds on SEL rates even in the absence of a simple model capturing trends and variability. In the next section, we use these relations as part of a SEL risk management methodology.

VII. Data-Driven SEL Risk Management

The insights derived from the JPL and CERN databases are useful when managing SEL-related risks. First, [4] and the additions to it from the JPL database suggest that roughly 50% of CMOS parts not specifically hardened against SEL will be susceptible to it, and further that 50% of SEL susceptible parts can fail destructively. Moreover, several of the parts in the CERN database have SEL rates as high as weeks to months between SEL, even in benign environments such as the International Space Station. The potential risks posed by SEL are not negligible. However, the datasets are useful not merely for illustrating the risks but also for managing them.

For example, if an application requires a device that is SEL immune, the 50% SEL rate for unhardened parts means that one must test ≥4 candidate devices to have >90% chance ($1-(0.5)^4$>93%) of finding at least one that meets that requirement. On the other hand, since ADCs and DACs tend to latch up 70% of the time, the number of candidate devices needed to have 90% confidence of at least one being SEL immune is ≥7.

Fig. 6 shows that a SEE test with LET as low as 30 MeVcm^2/mg is sufficient to identify 90% of SEL susceptible parts, and any that are missed will have SEL rates less than once in 10.5 years with 90% confidence (using the model (4) above and the bounding rate from (5) for LET=30 MeVcm^2/mg).

In some cases, the bound the bounding rate (5) imposed by a worst-case step-function will be deemed too conservative. In this case, one can use the analysis of section VI and bound the rate (for example) at a 90% WC LET_0 and 90% WC σ vs. LET. This reduces the rate for a SEL test with ion LET=30 MeVcm^2/mg to once in 16 years rather than once in 10.5 years.

However, assuming a 90% WC LET and a 90% WC σ vs. LET may still be deemed too conservative. Moreover, the dependence of the effect of *w* and *s* on LET_0 complicates defining the confidence level of the resulting rate. One can instead find a rate corresponding to a given confidence (e. g. 90 % WC) by sampling over the entire range for both LET_0 and the corresponding *r* distirbution, and then selecting the rate for the desired quantile (e.g. the 90% WC rate is exceeded by only 10% of rates in the sample space). Fig. 9 illustrates the quantiles from 1% to 99% for limiting cross sections from 10^{-7} to 10^{-1} cm^2. Fig. 10 repeats the process, this time as a function of LET_0 (observed, estimated or bounding) for values 2, 5, 10, 30, 40 and 55 MeVcm^2/mg. For LET=30 MeVcm^2/mg, this further reduces the 90% WC rate from once in 16 years to once in 25.7 years. The above techniques are useful for bounding either part-level or system-level rates. As test data become available, rates can be refined, and the system analyses updated with more specific rates for each part.

Usually, in testing, it is easiest to determine σ_s, as this requires only a single, high-fluence run at a sufficiently high LET. However, there remains the question of what constitutes a sufficiently high LET to determine σ_s with confidence. In general, σ curves with large Weibull width *w* pose the greatest difficulty in determining σ_s. If *s* and LET_0 are both large, this can also pose issues, since curves with large *s* rise slowly initially, before saturating rapidly near $LET_0 + w$. However, high values of LET_0, *w* and *s* all lower SEE rates, so moderate errors in estimating σ_s are unlikely to drive system-level SEL rates.

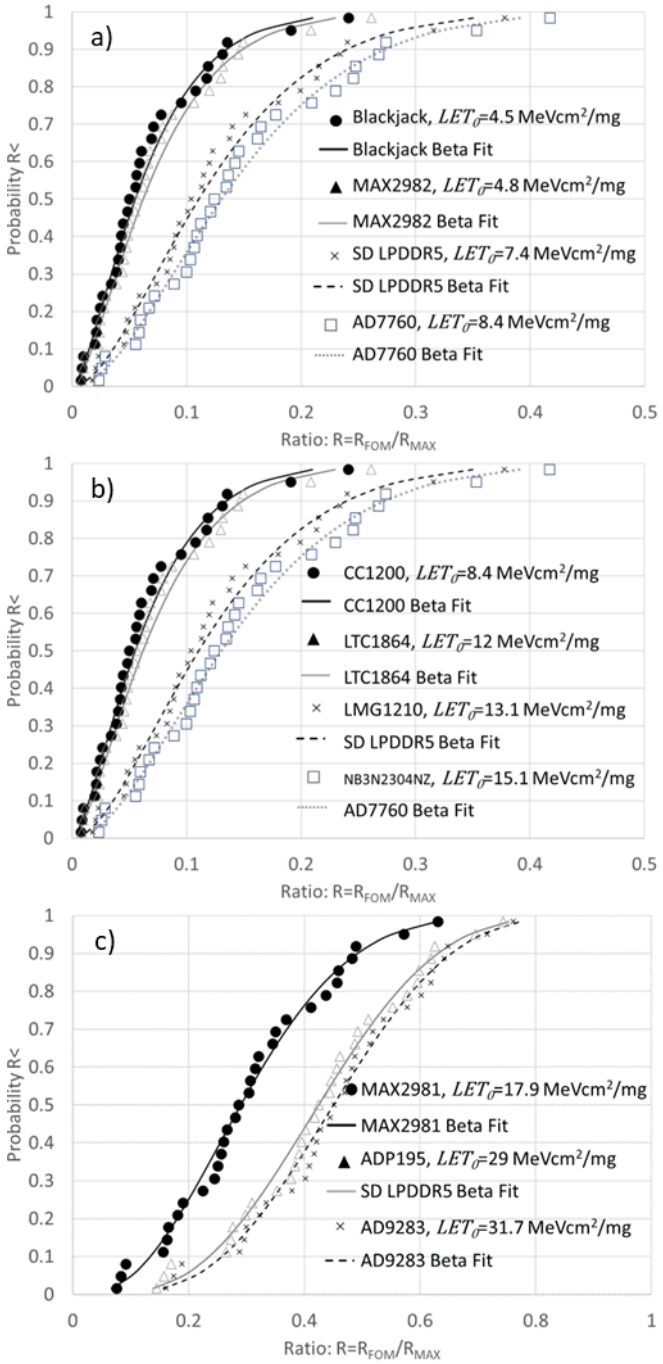

Fig. 7. Ratios of representative FOM rate estimates (using *w-s* pairs from Fig. 3) to worst-case bound for a) the 4 parts in Table II with the lowest values for LET_0; b) the next 4 lowest values for LET_0; and c) the 3 highest values for LET_0. Also shown are the best fits of the 31 FOM rate ratios for each part to a β distribution.

Taking the *w-s* pairs in Fig. 3 as representative of the rising behavior of σ vs. LET for SEL, and assuming LET_0 lies within below the 90% confidence limit for the model given by (4), we determined highest LET required to ensure σ vs. LET reaches at least 10%, 30% 50% and 90% of saturation for curves that result in an SEL rate of at least 10^{-6} per day in geostationary orbit. Fig. 11 shows the LET at which the last part among those in Fig. 3 reaches the % saturation (worst case LET) as well the LET where at least 90% of the parts have reached the % saturation (the 90% WC LET). What this means is that for an SEL cross section (or upper limit) at a given test LET, dividing by the corresponding percent saturation in Fig. 11 is likely to bound σ_s, while dividing by the 90% WC saturation yields ~90% confidence of bounding σ_s. These bounding values can then be fed into (4), and the rate bounded (either very conservatively using (5) or using the techniques developed above to bound at a known confidence).

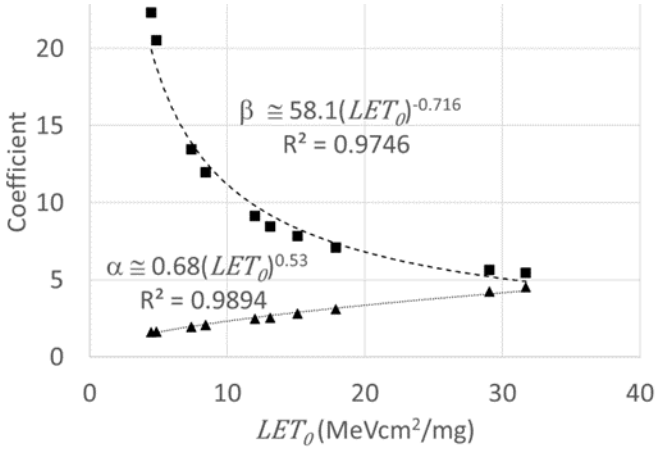

Fig. 8. The parameters of the β distributions fit to rate ratios in Fig. 7 follow power laws in LET_0 to a very good approximation.

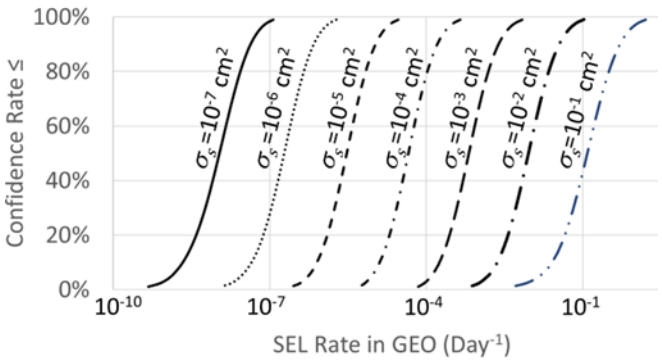

Fig. 9. Bounding SEL rate versus confidence for various limiting cross sections assuming the distribution of $LET_0(\mathrm{CL}|\sigma_s)$ given in (4).

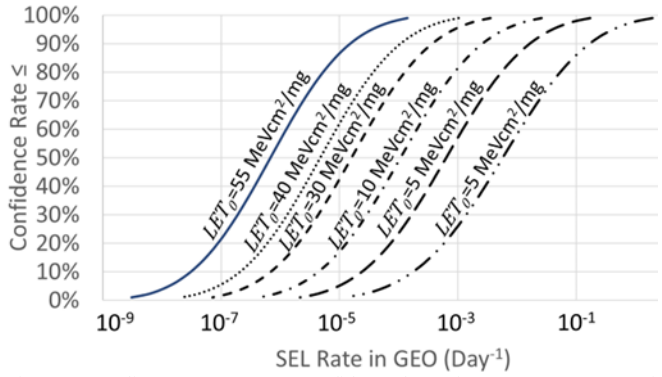

Fig. 10. Bounding SEL rate versus confidence for various onset LETs assuming the distribution of $\sigma_s(\mathrm{CL}|LET_0)$ given in (3).

VIII. Discussion and Future Work

The techniques developed here can provide meaningful bounds on SEL rates even with limited σ vs. LET or even bounding test data. However, they are predicated on the data in

the CERN and JPL databases being representative of the parts under consideration. The fact that most of the data were compiled during testing for a broad variety of space missions suggests that the data are consistent with the devices currently being considered for such missions. Moreover, Fig. 4 suggests that the basic susceptibilities have changed little over the last two decades, suggesting the data will remain representative for the foreseeable future. Another issue with this work is that—like all empirical trends—it is based on a finite dataset. With the addition of the 11 parts in Table II, the dataset is supported by 68 randomly selected (to the extent possible) parts. If the characteristic "supporting the trend" is viewed as a binomial variable, 68 parts supporting the trend with none in the "nonsupporting-" category suggests with 90% confidence that the non-supporting mode contains less than 3.4% of all parts. These results assume there is no data selection bias for parts that make it into the dataset. However, whether the goal is investigating such biases or improving model accuracy, the remedy is adding more data as they become available.

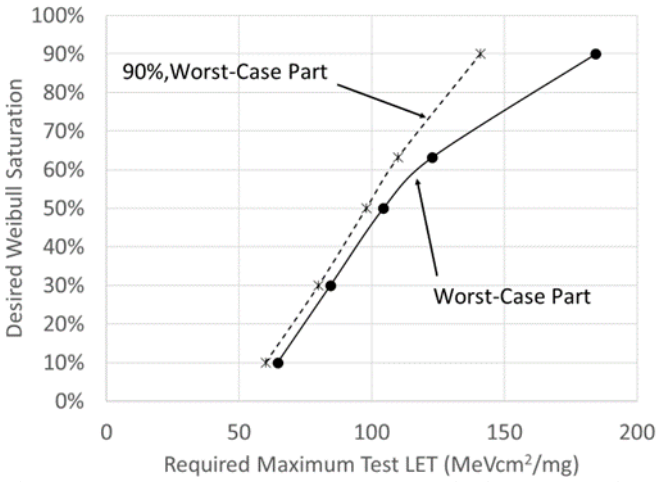

Fig. 11. Because some σ vs. LET curves saturate slowly, one cannot be sure that a single LET measures the true saturated cross section. By dividing the measured cross section at the highest test LET by the corresponding percentage, one can be assured σ_s is bounded.

Other outstanding issues to be resolved include the risks posed by potential latent damage [13,14] in parts exhibiting "nondestructive" SEL. If latent damage proves to be rare, or if it is easily detected post testing, this would increase the confidence with which parts susceptible to nondestructive SEL could be used. One goal in the review of JPL data was to search for parts potentially susceptible to latent damage. These parts will be investigated in a study funded by the NASA Engineering and Safety Center (NESC) with results to be published later.

The models discussed here ((3) and (4)) also suggest additional work to be done. In addition to growing the dataset, there is also the question is how closely σ_s must be estimated to yield meaningful bounds on the SEL rate. The last paragraph in section VII illustrates the difficulty of being certain a "high-LET" ion truly measures σ_s. However, testing with a maximum LET of 80 MeVcm2/mg is sufficient to reach 30% of saturation for ~90% of parts. Is dividing the measured cross section at 80 MeVcm2/mg by 0.3 sufficient for a bounding rate estimate?

Another approach that has yet to be investigated is whether the techniques outlined above can be implemented in conjunction with laser screening of parts for SEL susceptibility [19]. Significant progress has been made in translating laser threshold energy levels into onset LET_0 estimates [20-24]. On the other hand, it is difficult and time-consuming to measure σ_s with a laser. Using (3) would allow rate to be bounded based on a laser measurement of LET_0.

IX. Conclusion

The severe consequences of SEL, the prevalence of unhardened CMOS, the high incidence of susceptibility, and the high SEL rates for some parts combine to place this failure mode among the most significant obstacles to the use of state-of-the-art technologies in high-reliability applications. Moreover, the usual approaches to assess susceptibility prior to heavy-ion testing (analysis of SEL data for similar parts, proton testing, etc.) have proven ineffective.

Rather than attempt a priori prediction, the current work looks in large, diverse databases of susceptible parts for trends that can be combined with limited test data specific to parts under qualification to bound risk for those parts. Here we examined the CERN database [7] and the JPL database. With over 300 entries (both positive and negative test results), the JPL database was used to determine %susceptible, and how the proportion varies with part type, vendor, date, etc.

In [7], the CERN database was used to develop a model relating σ_s and LET_0, such that if σ_s is determined, LET_0 can be bounded with a desired confidence (and vice versa). This relation was used to develop a conservative approach to bounding SEL rates with little data, as a basis for a Bayesian prior for under-constrained SEL σ vs. LET and in a method for analyzing SEL susceptibilities for systems of varying complexity (e.g. # of potentially susceptible parts).

In this work, we looked at how Weibull parameters w and s affect σ vs. LET and the resulting rates. Taking the broad range of behaviors represented by the 31 w-s pairs in the CERN database as representative for SEL in unhardened CMOS, we developed a method to bound SEL rates at a known confidence given only σ_s or LET_0. Not only does this make it possible to bound risk with minimal heavy-ion SEE data, it may allow SEL rates to be bounded using pulsed laser testing if equivalency between LET and laser pulse energy can be determined.

We have also illustrated the complementary nature of different databases. The JPL database provides additional data that support the trends observed in the CERN database. The parameter distributions in the CERN database in turn allow the quality of the data in the JPL database to be assessed and even improved. For instance, for the parts in the JPL database tested only up to a maximum test LET of 26, 37 or 42, MeVcm2/mg, one may wonder how likely it is that testing to higher LET would reveal a hidden SEL susceptibility. If we take the CERN LET_0 data as representative of SEL susceptible parts, Fig. 7 can provide an answer. Similarly, Fig. 11, based on the CERN w-s data suggests σ_s may be bounded even if there are too few LETs in the cross section curve to establish saturation.

The JPL data also provide an archive in which one can look for parts that elucidate risks associated with latent damage or other gaps in our knowledge of SEL so these phenomena can

be studied and the gaps filled. The studies carried out here illustrate the potential that larger databases hold for improving understanding and assessment methodologies for radiation-related risks.

X. References

[1] T. E. Page and J. M. Benedetto, "Extreme latchup susceptibility in modern commercial-off-the-shelf (COTS) monolithic 1M and 4M CMOS static random-access memory (SRAM) devices," IEEE Radiation Effects Data Workshop, 2005., Seattle, WA, USA, 2005, pp. 1-7.

[2] F. Irom and S. G. Agarwal, "Compendium of Single-Event Latchup and Total Ionizing Dose Test Results of Commercial Digital to Analog Converters," 2015 IEEE Radiation Effects Data Workshop (REDW), Boston, MA, USA, 2015, pp. 1-8.

[3] R. L. Ladbury and M. J. Campola, "Bayesian Methods for Bounding Single-Event Related Risk in Low-Cost Satellite Missions," in IEEE Transactions on Nuclear Science vol. 60, no. 6, pp. 4464-4469, Dec. 2013.

[4] G. R. Allen et al., "2017 compendium of recent test results of single event effects conducted by the jet propulsion Laboratory's radiation effects group," 2017 IEEE Radiation Effects Data Workshop (REDW), pp. 7–16, 2017.

[5] A.E. Rudenkov, A.O. Akhmetov, D.V. Bobrovsky, A.I. Chumakov, A.V. Yanenko and V. M. Uzhegov, "The prediction for single event latchup sensitivity parameters of digital CMOS ICs based on its technological features," 2017 IEEE 30th International Conference on Microelectronics (MIEL), Nis, Serbia, 9-11 October 2017, pp. 287-290

[6] R. Ladbury, M. Bay and J. Zinchuk, "Threats to Resiliency of Redundant Systems Due to Destructive SEEs," in IEEE Transactions on Nuclear Science, vol. 68, no. 5, pp. 970-979, May 2021.

[7] R. Ladbury, "Under-Constrained SEE Data: Implications for Estimating and Bounding SEE Rates," in IEEE Transactions on Nuclear Science, vol. 71, no. 4, pp. 680-689, April 2024.

[8] C. C. Foster, P. M. O'Neill and C. K. Kouba, "Risk Assessment Based on Upset Rates from High Energy Proton Tests and Monte Carlo Simulations," in IEEE Transactions on Nuclear Science vol. 55, no. 6, pp. 2962 – 2969, Dec. 2008.

[9] A. H. Johnston, G. M. Swift, and L. D. Edmonds, "Latchup in Integrated Circuits from Energetic Protons," in IEEE Transactions on Nuclear Science, vol. 44, no. 6, December 1997

[10] R. García-Alía et al., "Simplified SEE Sensitivity Screening for COTS Components in Space," in IEEE Transactions on Nuclear Science, vol. 64, no. 2, pp. 882-890, Feb. 2017.

[11] R. Ladbury, L., J. -M. Lauenstein and K. P. Hayes, "Use of Proton SEE Data as a Proxy for Bounding Heavy-Ion SEE Susceptibility," in IEEE Transactions on Nuclear Science, vol. 62, no. 6, pp. 2505-2510, Dec. 2015.

[12] R. L. Ladbury and J. -M. Lauenstein, "Evaluating Constraints on Heavy-Ion SEE Susceptibility Imposed by Proton SEE Testing and Other Mixed Environments," in IEEE Transactions on Nuclear Science, vol. 64, no. 1, pp. 301-308, Jan. 2017

[13] H. N. Becker, T. F. Miyahira and A. H. Johnston, "Latent damage in CMOS devices from single-event latchup," in IEEE Transactions on Nuclear Science, vol. 49, no. 6, pp. 3009-3015, Dec. 2002.

[14] A. N. Tsirkov, D. V. Bobrovsky, A. A. Pechenkin, A. I. Chumakov and G. S. Sorokoumov, "Latent Single-Event Latchup-induced damage in Complementary Metal-Oxide-Semiconductor," 2018 18th European Conference on Radiation and Its Effects on Components and Systems (RADECS), Goteborg, Sweden, 2018, pp. 1-4.

[15] A. N. Tsirkov, "Methods of catastrophic failure prevention during the SEL-sensitivity estimation of IC," 2022 Moscow Workshop on Electronic and Networking Technologies (MWENT), Moscow, Russian Federation, 2022, pp. 105-108.

[16] A. Yanenko, "Qualitative Risk Assessment in the Application of Circuit-based Protection Against SEL in Space Electronics," 2022 Moscow Workshop on Electronic and Networking Technologies (MWENT), Moscow, Russian Federation, 2022, pp. 115-118.

[17] M. Andjelkovic, V. Petrovic, Z. Stamenkovic, G. Ristic and G. Jovanovic, "Simulation-Based Analysis of the Single Event Transient Response of a Single Event Latchup Protection Switch," 2015 IEEE 18th International Symposium on Design and Diagnostics of Electronic Circuits & Systems, Belgrade, Serbia, 2015, pp. 255-258

[18] Petersen, E. L., "The SEU Figure of Merit and Proton Upset Rate Calculations," IEEE Trans. Nucl. Sci., Vol. 45, No. 6, p. 2550-2562, 1998.

[19] D. Mcmorrow et al., "Laser-Induced Latchup Screening and Mitigation in CMOS Devices," in IEEE Transactions on Nuclear Science, vol. 53, no. 4, pp. 1819-1824, Aug. 2006.

[20] J. M. Hales, A. Ildefonso, A. Khachatrian, G. R. Allen and D. McMorrow, "Quantitative Laser Testing for Predicting Heavy-Ion SEE Response—Part 2: Accurately Determining Laser-Equivalent LET," in IEEE Transactions on Nuclear Science, vol. 71, no. 4, pp. 641-653, April 2024.

[21] M. Hales et al., "New Approach for Pulsed-Laser Testing That Mimics Heavy-Ion Charge Deposition Profiles," in IEEE Transactions on Nuclear Science, vol. 67, no. 1, pp. 81-90, Jan. 2020

[22] A. Ildefonso, J. M. Hales, A. Khachatrian, G. R. Allen and D. McMorrow, "Quantitative Laser Testing for Predicting Heavy-Ion SEE Response—Part 1: Metrics for Assessing Response Agreement," in IEEE Transactions on Nuclear Science, vol. 71, no. 4, pp. 626-640, April 2024

[23] M. Hales, A. Ildefonso, A. Khachatrian, G. R. Allen and D. McMorrow, "Quantitative Laser Testing for Predicting Heavy-Ion SEE Response—Part 2: Accurately Determining Laser-Equivalent LET," in IEEE Transactions on Nuclear Science, vol. 71, no. 4, pp. 641-653, April 2024

[24] M. Mauguet et al., "Single-Event Latchup in a CMOS-Based ASIC Using Heavy Ions, Laser Pulses, and Coupled Simulation," in IEEE Transactions on Nuclear Science, vol. 66, no. 7, pp. 1516-1522, July 2019.